

SEISMIC RETROFIT OF VULNERABLE BUILDINGS IN SPAIN WITH HYSTERETIC ENERGY DISSIPATORS

D. Domínguez, F. López-Almansa, A. Benavent-Climent

Abstract

In Spain, there are numerous vulnerable buildings, such as reinforced concrete frames with waffle slabs or wide beams. The use of hysteretic energy dissipators for seismic protection of wide-beam buildings is proposed. This study focusses in 3 and 6-story representative buildings; each building is designed for no, moderate and mid seismicity (design PGA 0.0 g, 0.12 g and 0.23 g, respectively). The mechanical parameters of the dissipators are selected from two approaches: an algorithm aiming to obtain uniform cumulated plastic ductility along the height of the building and a simpler approach where the yielding forces of each dissipative device are chosen proportional to those induced by the equivalent static forces in the Spanish design code. The suitability of the proposed solutions is assessed through dynamic analyses for representative seismic records; the performance criteria are the reduction of the interstory drift, of the base shear, of the absolute accelerations, and of the cumulated plastic displacements in the structure and in the dissipators. Three cases are compared: bare frame (building without any bracing), protected frame (building with dissipators) and braced frame (building with rigid connections instead of dissipators). This research belongs to a wider initiative that includes testing and practical applications.

Keywords: seismic retrofit, reinforced concrete buildings, wide beams, energy dissipators

Resumen

En España existen numerosos edificios vulnerables, como los de pórticos de hormigón armado con losas reticulares y con vigas planas. Se propone el uso de disipadores de energía histeréticos para protección sismorresistente de edificios de vigas planas. El estudio se centra en edificios representativos de tres y seis plantas; cada edificio se proyecta para sismicidad nula, moderada y media (aceleración de proyecto 0,0 g, 0,12 g y 0,23 g, respectivamente). Los parámetros mecánicos de los disipadores se eligen según dos formulaciones: un algoritmo orientado a lograr en éstos la mayor uniformidad posible, a lo largo de la altura del edificio, de la ductilidad plástica acumulada y un procedimiento más sencillo en que las fuerzas de plastificación de cada disipador es proporcional a las fuerza generada en este dispositivo por las fuerzas estáticas equivalentes según la normativa española. El rendimiento de las soluciones propuestas se evalúa, a partir de cálculos dinámicos para registros sísmicos representativos, en términos de reducción de los desplazamientos máximos entre plantas, de la fuerza de interacción entre la estructura y el terreno, de las aceleraciones absolutas en las plantas y de los desplazamientos plásticos acumulados en la estructura y en los disipadores. Para ello se comparan tres alternativas: edificios sin proteger, edificios protegidos con disipadores y edificios con arriostramientos rígidos. Esta investigación forma parte de un proyecto más amplio, que incluye ensayos experimentales e iniciativas para la aplicación de los resultados obtenidos.

Palabras Clave: rehabilitación sísmica, edificios de hormigón armado, vigas planas, disipadores de energía

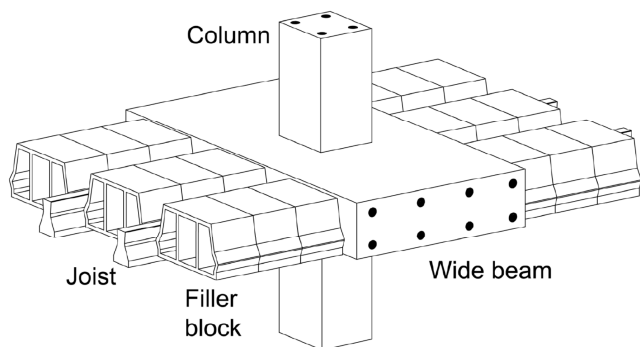
1 Introduction

In Spain, there are numerous vulnerable buildings, such as Reinforced Concrete (RC) frames with two-way waffle slabs or one-way wide-beam slabs. Additionally, many regions of Spain possess relevant seismicity, having been clearly underestimated, as pointed out by the recent Lorca earthquake (11-05-2011), the strongest event ever recorded in Spain. This lack of concern about the seismic risk has generated loose design codes, weak seismic knowledge of the structural designers and low enforcement of the existing regulations. Given this situation, a joint research initiative started about ten years ago; its final objective is to reduce the seismic risk of those buildings by using energy dissipative devices. Regarding the wide-beam buildings, earlier works consisted of experiments aiming to characterize the hysteretic behavior of wide beam-columns joints [Benavent-Climent 2007, Benavent-Climent et al. 2009a, b]; next researches consisted of theoretical studies on the vulnerability of code-compliant wide-beam buildings [Benavent-Climent and Zahran 2010] and of non-code-compliant wide-beam buildings [Domínguez 2012, López-Almansa et al. 2013]. Recent works [Benavent-Climent et al. 2013, Domínguez et al. 2014] discuss the behavior, under the Lorca input, of wide-beam buildings located in Lorca and of non-code compliant wide-beam buildings located in Spain, respectively. This work is a part of this research activity; the goal is proposing retrofit strategies based on energy dissipators, for any type of wide-beam buildings located in any region of Spain.

Wide-beam buildings are extremely common in Spain and other close countries, such as France and Italy. The buildings have a concrete framed structure with one-way slabs as the primary system. The wide beams constitute the distinctive characteristic, their width being greater than that of the supporting columns and their depth being equal to that of the rest of the slab, thus providing for a flat lower surface, which facilitates construction of the slabs and layout of the facilities. Figure 1 displays an image and a sketch of a one-way slab with wide beams.



(a) Lower view of a one-way slab with wide beams



(b) Wide beam-column joint

Figure 1 – Wide-beam slabs

Beyond being highly widespread in Spain, this construction typology has been chosen because of its apparent high seismic vulnerability [Domínguez 2012, López-Almansa et al. 2013]. In the direction of the wide beams, the following weaknesses can be presumed:

- The lateral strength and stiffness of the building are low, mainly because the effective depth of the beams is small (as compared to that of conventional beams).
- The ductility of the wide beams is low since the amount of reinforcement has to be high (commonly ranging between 2% and 6%), to compensate for insufficient effective depth.
- The strut compressive forces developed inside the column-beam connections are considerable, due to the low height of the beams.

- Since the beams are wider than the columns, a relevant part of the longitudinal reinforcement of the beams lies beyond the vertical projection of the columns (Figure 2.b). Hence, the contribution of such outer zones of the beams to the bending resistance of the beam-column connections is unreliable, since the moment transfer from beam to column relies on a torsion mechanism [Benavent-Climent et al. 2009a, b], and the beams are not designed to sustain torsion (i.e. they do not have any torsion reinforcement).

In the orthogonal direction, the lateral seismic behavior might be even worse, since the only members of the slabs that contribute to the lateral resistance of the buildings are the joists and the façade beams [Domínguez 2012, López-Almansa et al. 2013].

Two prototype buildings, 3 and 6-story, are chosen to represent the vast majority of the edifices with wide beams located in Spain. For the purpose of this study, Spain is divided into three seismic zones in terms of the design ground acceleration [NCSE-02 2002] (a_b): low or no seismicity ($a_b < 0.08$ g), moderate seismicity ($0.08 \text{ g} \leq a_b < 0.16$ g) and medium (or mid) seismicity ($0.16 \text{ g} \leq a_b$). Both prototype buildings are designed for each of the three seismic zones. The buildings in the low seismicity region are assumed to have been designed without any seismic provision (e.g. non-code-compliant buildings, $a_b = 0.0$ g). The buildings in the moderate seismicity region are located in Lorca ($a_b = 0.12$ g) and the buildings in the medium seismicity region are located in Granada ($a_b = 0.23$ g). Given the low lateral resistance of the main frames, the cooperation of the masonry infill walls is accounted for in assessing their actual lateral capacity and seismic behavior; for each prototype building, three wall densities are considered: no walls, low wall density and high wall density.

2 Wide-beam buildings in Spain

2.1 *Introductory remarks*

As stated in the Introduction, wide-beam buildings are extremely common in Spain, even in the most seismic-prone areas. Two three-story and four six-story prototype buildings are selected to represent the vast majority of the actual ones. The characteristics of the prototypes are determined from an extensive survey among experienced designers [Domínguez 2012]. Each of these edifices is structurally designed for three different seismic conditions in Spain: no seismicity, moderate seismicity and medium seismicity. Next subsection describes the overall characteristics of such constructions and the two other subsections describe, respectively, the particular characteristics of the buildings designed for “no seismicity” and for “moderate and medium seismicity”.

2.2 *Prototype buildings*

Two 3- and 6-story and 4-bay prototype buildings are chosen to represent the vast majority of the edifices with wide beams located in Spain; see Figure 2. Figure 2.a and Figure 2.b display overall views of the 3-story and 6-story buildings, respectively; both sketches show that the considered buildings are regular and symmetric; hence, no relevant twisting effects are expected. Although there are wide-beam buildings with markedly asymmetric configurations, they are relatively scarce and there are no clear common patterns; for this reason, asymmetric buildings are not considered in this study. Figure 2.c displays a plan view of a slab; that sketch highlights that in the x direction every one-way slab contains five wide beams while in the y direction there are two (outer) façade beams and three (inner) joists that are coplanar with columns. Figure 2.d and Figure 2.e display cross-sections of a wide beam and of secondary beams, respectively; those sketches show that the wide beams are wider than the columns, whereas the width of the façade beams is equal to the one of the columns. Figure 2.e also shows that the joists are semi-prefabricated, being composed of a lower “sole” and a “truss-type” naked reinforcement; since pre-stressed, pre-fabricated beams are also commonly employed as

joists, they have been likewise considered in our analyses. Figure 2.d shows that the top splice bars guarantee the continuity of the joists. The first floor is 4 m high while the upper floors are 3 m high; the span-length is 5 m in both directions.

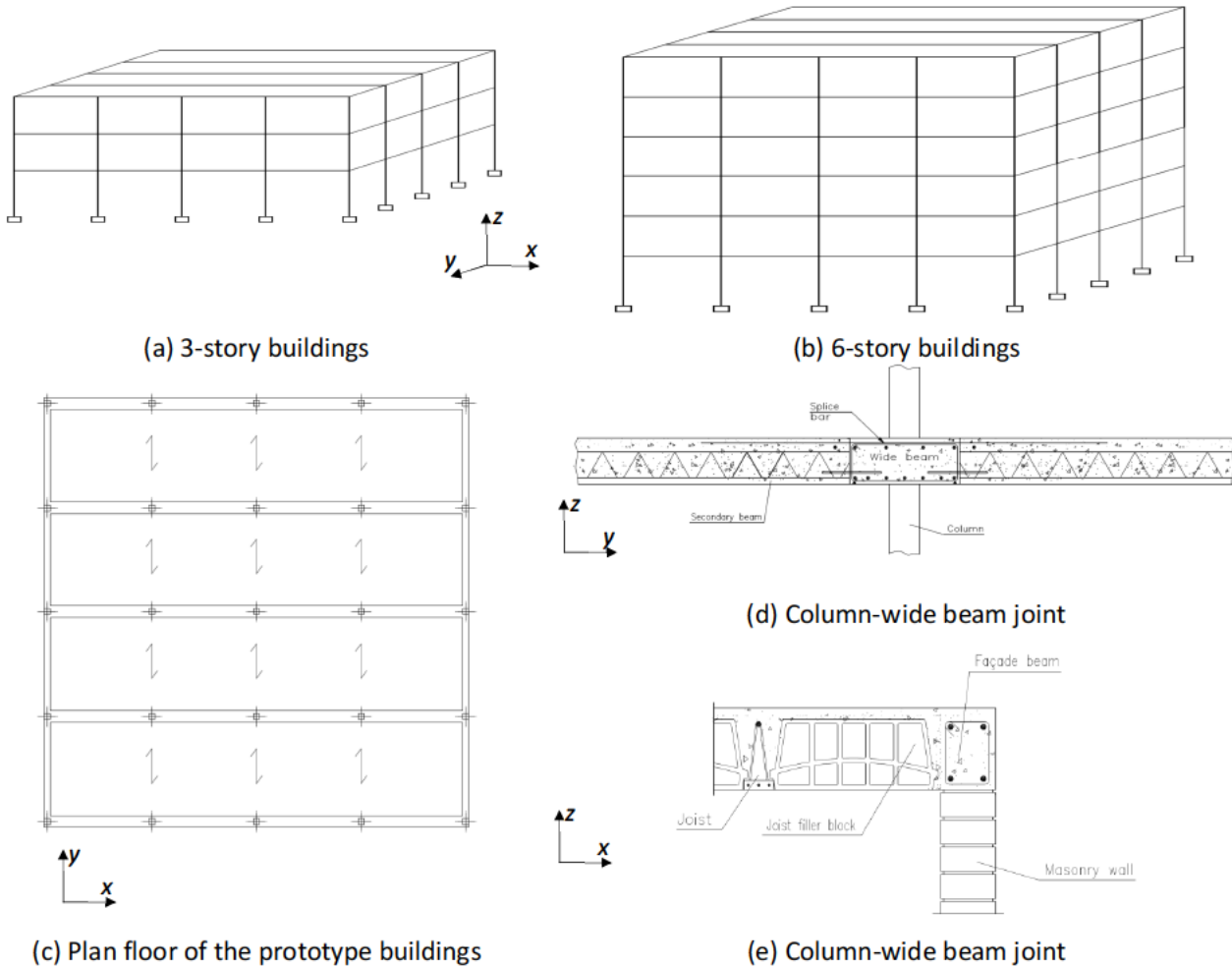


Figure 2 – Three and six-story prototype buildings

Each of the prototype buildings is designed, according to the current Spanish code [NCSE-02 2002], for three seismic conditions: no seismic provision (design PGA 0.0 g), moderate seismicity (design PGA 0.12 g, as in Lorca) and medium seismicity (design PGA 0.23 g, as in Granada). Noticeably, the buildings without seismic design can correspond to any region of Spain in the period 1974-1994; i.e. prior to the approbation of the 1994 seismic design code [NCSE-94 1994]. Basically, the buildings for Lorca and Granada are intended to correspond to the period 2002-present; that is, after the approbation of the 2002 seismic design code [NCSE-02 2002].

For buildings without seismic consideration, the characteristic value of the concrete compressive strength is 17.5 MPa; the top concrete layer of the slabs is 4 cm deep and is not reinforced (Figure 2.d and Figure 2.e). The steel type is AEH 400 S [EH-80 1980]; its yielding point and ultimate stress are 410 MPa and 530 MPa, respectively, and the ultimate strain is 14%.

The prototype buildings in moderate and medium seismicity regions are designed according to the current Spanish [NCSE-02 2002] and European [EN 1998 2004] seismic design codes. In both cases the analyses consisted of determining static equivalent forces in both horizontal directions. The static forces were obtained from the response spectra for 5% damping and design seismic accelerations

0.12 g (Lorca) and 0.23 g (Granada); according to Spanish regulations, these accelerations correspond to stiff soil and to a 500 year return period. For each building, the four major soil types included in the two codes have been considered. The Eurocode denotes them as soil A (rock, $v_{s,30} > 800$ m/s where $v_{s,30}$ is the shear wave velocity averaged over the top 30 m of soil), B (stiff soil, $360 < v_{s,30} < 800$ m/s), C (soft soil, $180 < v_{s,30} < 360$ m/s) and D (very soft soil, $v_{s,30} < 180$ m/s). For these soil types, the right/left-hand edges of the response spectra plateau corresponds to periods ranging from 0.1/0.4 s to 0.2/0.8 s in Spanish regulations [NCSE-02 2002] and from 0.05/0.25 s to 0.10/0.30 s in European regulations [EN 1998 2004]. It was found that in soils B, C and D the structural solution of frames with wide beams is not feasible because it would require slabs of excessive depth and too massive columns; therefore, only soil A is considered. For soil A, the beams cannot be as wide as in the non-code-compliant buildings because of code limitations in the percentage of the top longitudinal reinforcement of beams that lie out of the projection of the column. The response reduction factor is assumed as $\mu = 2$ in the Spanish code and as $q = 1.5$ in the Eurocode, regardless of the wall density. No accidental eccentricity is considered in the derivation of the equivalent seismic forces. Comparison between the seismic forces prescribed by Spanish and European regulations shows them to be similar. The seismic structural design has been carried out trying to emulate the common practices in Spain; for this reason, the cooperation of the masonry infill walls has not been taken into consideration. The characteristic value of the concrete compressive strength is 25 MPa; the top concrete layer of the slabs is 5 cm deep and is reinforced (Figure 2.d and Figure 2.e) with a 15×15 cm wire mesh made with 5 mm diameter bars. The steel type is B 500 SD [EHE 2008] (high ductility); its yielding point and ultimate stress are 500 MPa and 575 MPa, respectively, and the ultimate strain is 16%.

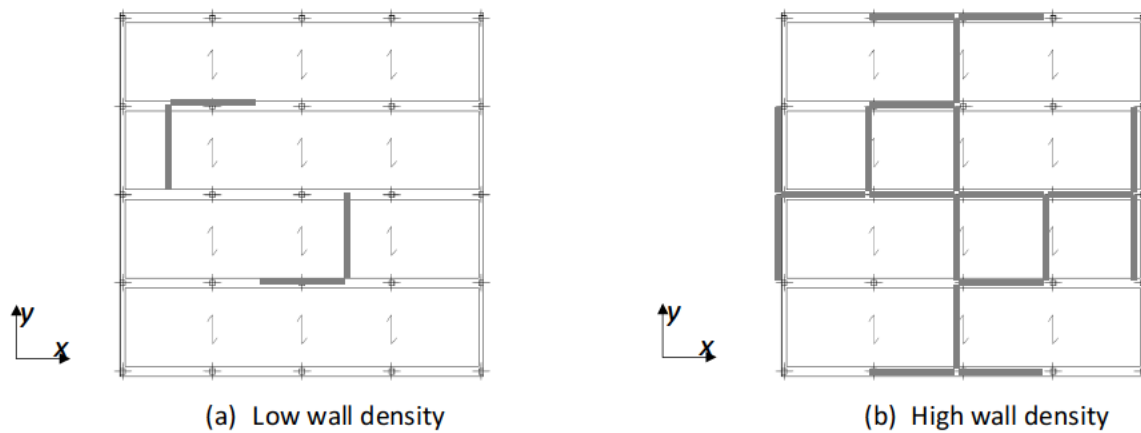


Figure 3 Infill walls layout

Since the prototype buildings possess only low lateral resistance, the cooperation of the infill walls cannot be neglected [Ricci et al. 2013]. In this study, however, only the contribution of walls made with “Group 2” brick units [EN 1996 2005] 12 cm thick was accounted for. The walls whose contribution is neglected are either the ones structurally detached from the main frame or those made of 4 cm thin bricks (Group 3 or 4 brick units). The walls of the first type are not considered because they are not affected by the drift motion of the main structure; the walls of the second type are neglected because their behavior is too brittle to allow the deformations required by the plastic strut-and-tie behavior [Martínez et al. 2001]. In the infill walls, the characteristic values of the brick and mortar strengths are, respectively, 12 and 8 MPa. For each of the six representative buildings three wall densities were considered: “no walls”, “low wall density” and “high wall density”. The first and second cases correspond to commercial buildings with light claddings, while the third case corresponds to houses. Figure 3 depicts typical layouts of the walls for the second and third cases.

Since the infill walls are placed symmetrically in both directions, the horizontal behavior will be also symmetric. All these walls are assumed to be continuous down to the foundation; yet the pilotis case (e.g. lack of walls in the first floor) has repeatedly shown to be extremely prejudicial [Ricci et al. 2013, Benavent-Climent et al. 2012, 2013], it has not been considered in this study because it was deeply analyzed in a previous work by some of the authors [Benavent-Climent et al. 2013]. The walls are 15 cm thick, of which 12 cm are for the bricks and 3 cm for the plaster coating. On each floor, it is assumed that the walls occupy the entire height; therefore, the possible short column effect is not taken into account.

Table 1 describes the main characteristics of the prototype buildings. In the notation B3-0.0g, “3” refers to the number of floors and 0.0g corresponds to the design PGA. The fundamental periods correspond, respectively, to the direction of the wide beams and to the orthogonal one. Those periods were determined from the numerical models of the buildings described in the next section, to be considered for the push-over and dynamic analyses. The last column contains the total weight of the buildings corresponding to the loading combination $G + 0.3 Q$ (G and Q represent the dead and live loads, respectively); the influence of the walls in the weight of the buildings was neglected [Domínguez 2012].

Table 1. Prototype buildings

Building	Floors / height (m)	First floor columns (cm)	Top floor columns (cm)	Wide beams ($b \times h$) (cm)	Weight ($G + 0.3 Q$) (kN)	Fundamental periods (x/y) (s)		
						No walls	Low wall density	High wall density
B3-0.0g	3 / 10	40 × 40	30 × 30	60 × 25	9770	0.585 / 1.037	0.264 / 0.285	0.126 / 0.128
B3-0.12g	3 / 10	40 × 40	30 × 30	50 × 35	10935	0.407 / 0.524	0.119 / 0.125	0.118 / 0.125
B3-0.23g	3 / 10	50 × 50	40 × 40	60 × 40	12005	0.241 / 0.302	0.117 / 0.119	0.110 / 0.114
B6-0.0g	6 / 19	50 × 50	30 × 30	60 × 25	20310	1.333 / 2.630	0.400 / 0.413	0.185 / 0.187
B6-0.12g	6 / 19	50 × 50	30 × 30	50 × 40	26542	0.686 / 1.109	0.251 / 0.280	0.150 / 0.178
B6-0.23g	6 / 19	60 × 60	40 × 40	60 × 40	28430	0.450 / 0.628	0.245 / 0.275	0.143 / 0.144

Comparison among the fundamental periods in Table 1 shows that the code-compliant buildings are significantly stiffer and that the cooperation of the walls increases visibly the stiffness.

3 Modeling of the dynamic behavior of the prototype buildings

3.1 Considered structural models

This section describes the model of the dynamic structural behavior of the prototype buildings. The analyses will be carried out with the program IDARC-2D, version 7.0 [Kunnath, Reinhorn 2010]. The nonlinear static and dynamic structural behavior of the buildings in each direction is described with 2D finite element models. Beams and columns were modeled with frame elements and the infill walls were modeled with compression-only bars joining adjacent floors. The diaphragm effect of the floor slabs is accounted for by rigid fictitious pin-ended bars connecting the outer nodes of the frames.

3.2 Modeling of the frames

The connections between the columns and the wide beams (x direction) and between the columns and the façade beams (y direction) were modeled as rigid since the reinforcement is assumed to be

satisfactorily anchored [Domínguez 2012]. Conversely, the connections between the columns and the joists (y direction) were modeled as rigid for negative bending moments yet are considered as ordinary hinges (pin connections) for positive bending moments since Figure 2.d shows that the lower reinforcement bars are not adequately anchored. The behavior of concrete and steel is described by classical uniaxial constitutive laws; the stress-strain diagram for steel is bilinear, with strain hardening while the one of concrete is a parabola-rectangle model where the tension strength is neglected [EN 1992 2003]. In the x and y frames, the nonlinear behavior is concentrated in plastic hinges located at both ends of each member; the length of each plastic hinge is estimated as half of the depth of the cross-section of the member [Reinhorn et al. 2009]. In the six considered buildings it was thoroughly checked that positive moment hinges did not form along the span of the beam [Domínguez 2012].

The hysteretic behavior of the plastic hinges of the columns, of the wide beams (x direction, see Figure 2 and Figure 3) and of the façade beams and the joists (y direction) is described by the polygonal hysteretic model (PHM) implemented in IDARC. The PHM model uses a non-symmetric monotonic envelope defined by the elastic stiffness K_e , the secant stiffness K_0 , the cracking moment M_c , the yielding moment M_y , the curvature-ductility factor μ_ϕ ; and four parameters that control the effects of stiffness degradation (HC), strength degradation (HBE, HBD) and pinching (HS). The meaning of these parameters can be found in [Reinhorn et al. 2009]. The moment M_y was determined according to [ACI 318-08 2008] and the obtained results were compared to those provided by the program Response 2000 [Bentz, Collins 1992], the agreement proving satisfactory. The cracking curvature was determined from the initial sectional stiffness K_e , calculated by classical linear analyses, accounting for the contribution of the reinforcement bars. The secant stiffness K_0 was calculated multiplying the initial elastic sectional stiffness of the gross sections by a factor γ that takes into account the effects of concrete cracking and axial force [Sugano 1968]. The parameters μ_ϕ , HC, HBE, HBD and HS were determined through a parametric study to give the best fitting with previous test results [Benavent-Climent et al. 2009a, b], in terms of maximum strength, initial stiffness and total energy dissipated. Good fittings were obtained with HBD = 0, HS = 0.2, μ_ϕ = 12, HC = 2, HBE = 0.6 for wide beams in exterior connections; and HBD = 0, HS = 0.2, μ_ϕ = 21, HC = 3.5, HBE = 0.4 for wide beams in interior connections. For the exterior columns HBD = 0, HS = 0.2, μ_ϕ = 3, HC = 1.8, HBE = 0.6, and for the interior columns HBD = 0, HS = 0.2, μ_ϕ = 3, HC = 3.1, HBE = 0.4 [Benavent-Climent and Zahran 2010]. The validity of these hysteretic parameters was further corroborated by the results of two dynamic shake table tests on one exterior and one interior wide beam-column subassemblies [Benavent-Climent 2007]). These values of the curvature ductility μ_ϕ are similar to those adopted in [Masi 2003] for flexible beams of post-1970 Italian RC frames designed only for gravity loads (μ_ϕ = 20). Further, they provide chord rotation ductility ratios close to those obtained in the tests. The assumed parameters for the façade beams (y direction) are equal to those of the exterior wide beams. For the joists, HBD = 0, HS = 0.2, HC = 3.5, HBE = 0.4; given the lack of experimental results, the ductility curvature was conservatively estimated as μ_ϕ = 4; it should be stressed that, since the contribution of the joists to the transverse lateral resistance is relatively low, it is expected that the overall behavior of the buildings in transverse direction (y) is not very sensitive to this parameter. In the columns, the interaction with the compressive axial force is taken into account [Reinhorn et al. 2009].

3.3 Modeling of the infill walls

The hysteretic behavior of the masonry infill walls is represented by Bouc-Wen models [Baber, Noori 1985]. Those models are characterized by two major parameters, i.e. the resistance and the initial stiffness. The resistance is obtained from tie-and-strut models, wherein two major failure modes are considered: diagonal strut compression and horizontal sliding along a course. In all the analyzed cases,

the resistance for the first failure mode was significantly smaller. The possible “short column” effects [Mehrabi et al. 1994] were not held to be relevant since the length of the columns that are in contact with the diagonal struts is rather small [Domínguez 2012]: for walls that are 3 m high and 5 m long it is 0.68 m, for walls that are 3 m high and 5.5 m long it is 0.72 m, for walls that are 4 m high and 5 m long it is 0.76 m, and for walls that are 4 m high and 5.5 m long it is 0.80 m. These values were obtained as suggested in [Paulay, Priestley, 1992] and correspond to non-code-compliant building (low seismicity regions). The parameters for the tie-and-strut models were estimated as indicated by the Eurocode 6 [EN 1996 2005]. As suggested in [Mostafaei, Kabeyasawa 2004], the initial stiffness is estimated as two times the ratio between the ultimate resistance and displacement. The post-peak behavior is modeled as non-existent.

The wall characteristic strength f_k and the secant longitudinal and transverse deformation moduli [Martínez et al. 2001] are

$$f_k = K f_b^{0.70} f_m^{0.30} = 0.45 \times 12^{0.70} \times 8^{0.30} = 4.781 \text{ MPa}$$

$$E = 500 f_k = 2391 \text{ MPa} \qquad G = 0.4 E = 956 \text{ MPa}$$

The value of coefficient K has been chosen according to the brick unit type (clay, group 2), the mortar (general purpose) and the presence of longitudinal joints. After these results, the chosen value of the design parameters are VYIW = 352 kN (lateral yield force), EAIW = 56 kN/mm (lateral initial stiffness) and MU = 15 (ductility).

The risk of brittle shear failure of the columns generated by the horizontal components of the diagonal compressive forces is contemplated, in a simplified way, by verifying that the columns fulfill the ductility requirement of the Spanish design code [EHE 2008]. Following a capacity-based design philosophy, the code prescribes that the columns should be able to resist, with a reasonable safety margin, the maximum demanding shear force compatible with the resisted plastic moments at the end sections of the columns; the resisted plastic moments are determined accounting for the actual demanding axial forces. Given the considered ductility ($\mu = 2$, subsection 2.2), the Spanish code indicates that the safety margin should be, at least 20%; in all the considered forces, the actual safety margin has been higher. Similar prescriptions are contained in the Eurocode 8 [EN 1998 2004].

3.4 Characteristics of the dynamic analyses

Time integration was done using the Newmark- β method [Newmark 1959]; the time step is 0.001 s and the damping is described by a 5% Rayleigh model. Given the high lateral flexibility of the considered buildings, second-order analyses were performed; in most of the cases the differences with the first-order analyses were small.

4 Proposed protection system

The proposed retrofit strategy consists of incorporating steel bracing members to each of the four façades (to obtain plan symmetry and torsion strength) and to each story (to obtain vertical uniformity). Figure 4 displays solutions with chevron (Figure 4.a) and diagonal (Figure 4.b) braces; in both cases, energy dissipators are installed as experiencing relevant strains under interstory drift motions. Figure 4 shows that, for chevron/diagonal braces, each bracing unit consists of the series combination of two braces and one/two energy dissipator/s. Although any type of dissipative device might be employed, only hysteretic dissipators (e.g. its dissipative behavior is based on plastification of metals, commonly steel) are considered in this research. This decision has been taken since those devices are cheap, robust, simple, and have repeatedly proven its efficiency and reliability; as well,

many devices have been proposed and a number of experiments, numerical simulations and applications have been reported.

In this study, three cases are compared: bare frame, protected frame and braced frame. The first case consists of the buildings without any bracing (Figure 2.a y Figure 2.b), the second one corresponds to the buildings with dissipators (Figure 4.a and Figure 4.b) and the third one is similar to the second case but replacing the dissipators with rigid connections between the steel braces and the top floor.

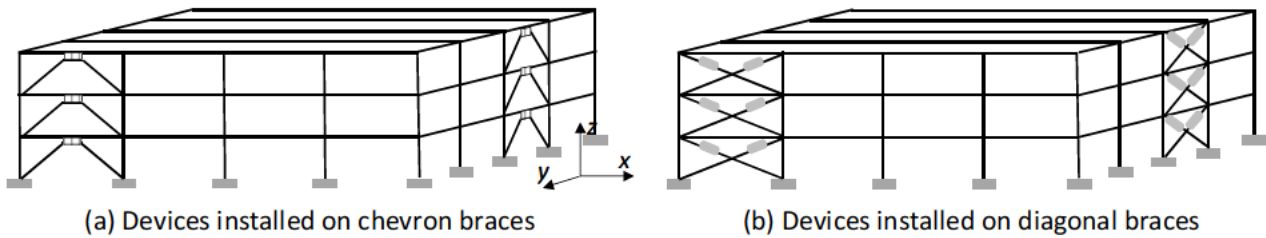


Figure 4 – Proposed retrofit strategies using energy dissipators

The monotonic behavior of the hysteretic devices is described with bilinear laws; the cyclic hysteretic behavior takes into account the Bauschinger effect in the reloading branches.

5 Design criteria for the hysteretic dissipative devices

The energy that can be dissipated in the whole building in a given direction cannot be obtained by merely adding the capacities of each story; it depends on the distribution, among the different stories, of the dissipated energy and on the accidental eccentricities between their centers of mass and rigidity. To cope with this issue, a number of formulations to select the variation, along the building height, of the design initial (elastic) stiffness and yielding forces of the hysteretic dampers have been proposed; in this paper, the approach in the work [Benavent-Climent 2011, 2014] is considered. This formulation is an energy-based procedure in which the required base shear force to be provided by the dampers is obtained by establishing the energy balance of the system, and the total lateral strength distribution (i.e. frame+dampers) is determined to provide a rather uniform distribution of the cumulative ductility η in each level along the building height. The later is achieved by adopting as lateral strength distribution the maximum shear-force distribution in an equivalent elastic undamped shear strut with similar lateral stiffness distribution along its height, subjected to a bilinear energy input spectrum. In this procedure, the earthquake hazard is characterized in terms of input energy and several seismological parameters (predominant period of the soil T_G , I_D index [Manfredi 2001], etc.) that take into account the proximity of the earthquake to the source.. The study has been carried out for the following conditions: building B3-0.12g in the main (x) direction (see Figure 2 and Table 1), near-fault inputs with dimensionless index $I_D = 7.5$ [Manfredi 2001], medium stiffness soil with predominant period $T_G = 0.52$ s, input energy in terms of equivalent velocity $V_D = 64.6$ cm/s and ratio between the hysteretic and input energies $V_E / V_D = 0.7$ [Akiyama 1985]. The value of V_D has been obtained from the reference [Benavent-Climent et al. 2002] for moderate seismicity regions of Spain, like Lorca. Table 2 displays the selected values of the stiffness and yielding forces of the dissipators; values in Table 2 represent all the devices located in a given direction (Figure 4). Noticeably, the stiffness coefficients correspond to the braces-devices assemblies.

Table 2. Design parameters of the dissipative devices

Floor No.	Initial stiffness (kN/mm)	Yielding force (kN)
1	1053	2679
2	736	2261
3	867	1486

The obtained values of the yielding forces of the dissipators are compared with those arising from the simpler formulation in [Foti et al. 1998]. This approach relies on representing the effect of the expected seismic action in terms of equivalent static forces; then, the yielding force at each story is selected as a given percentage of the corresponding internal shear forces in each set of dissipators in a given story and direction. The equivalent forces have been obtained according the Spanish design code [NCSE-02 2002] for a design peak acceleration equivalent to the EW component of the Lorca record (Figure 5.b). According to this formulation, the design values of the yielding force are 2929, 2234 and 1181 kN, respectively. Comparison with the values in Table 2 show a big coincidence.

6 Numerical results

The recent Lorca earthquake (11-05-2011) is the most severe seismic event ever recorded in Spain [IGN 2011], despite its rather moderate magnitude ($M_w = 5.1$; [IGME 2011]). This severity is mostly contributed by the extremely shallow hypocenter (the hypocentral depth is estimated as 2 km), by the high proximity between the epicenter and the city center (2.9 km until the seismologic station) and by the strong impulsive character of the registers. Figure 5 displays the most severe registered accelerograms [IGN 2011]; those inputs were recorded in a stiff soil site, almost rock-type.

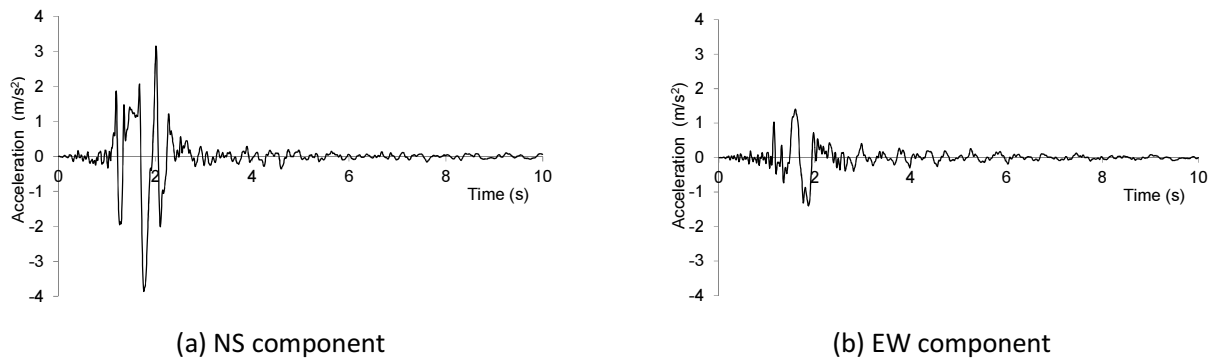
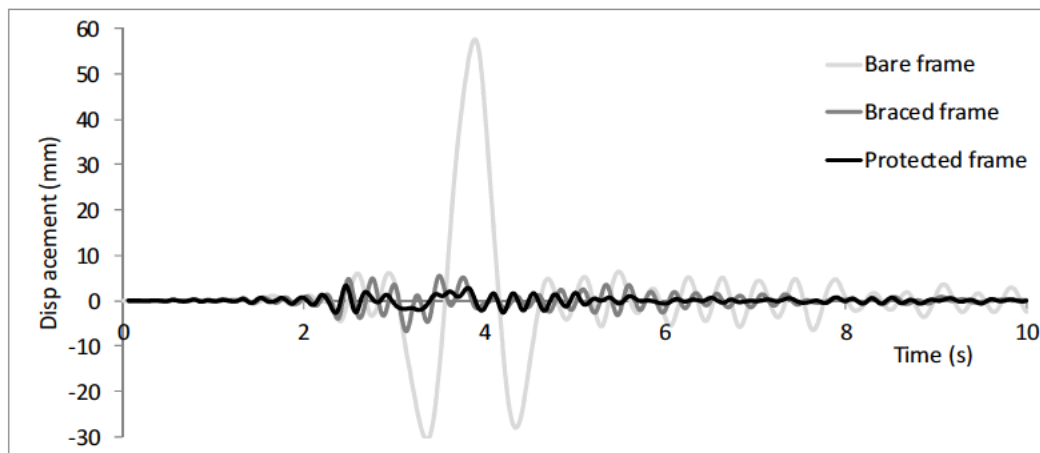
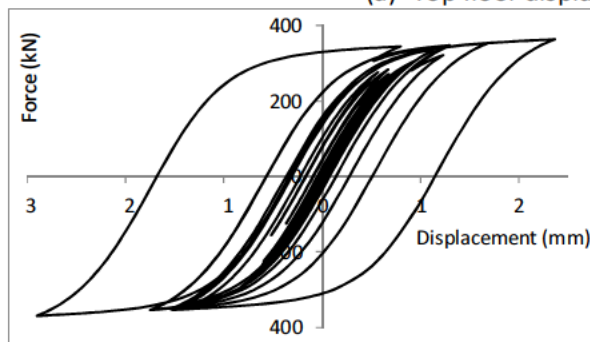


Figure 5 – Accelerograms of the Lorca earthquake (11-05-2011)

Preliminary results for the prototype building B3-0.12g in the x direction under the EW component of the Lorca record (Figure 5.b) are shown next. Chevron braces are considered (Figure 4.a). The parameters of the dissipators are taken from Table 2. As discussed in section 4, three cases are considered: bare frame, protected frame and braced frame. Figure 6 displays several response magnitudes; Figure 6.a represents the time-history of the top floor horizontal displacement, Figure 6.b shows the hysteresis loops of the sets of dissipators in the first floor, and Figure 6.c represents the time-history on the input energy. Plots from Figure 6.a show that the response of the protected frame is clearly smaller than the one of the bare frame; comparison with the response of the braced frame, shows a less intensive reduction. Figure 6.b shows a regular and expected behavior, with relevant encompassed area (e.g. dissipated energy). Figure 6.c confirms that the maximum input energy is reached at the end of the shaking.



(a) Top floor displacement time-history response



(b) Hysteresis loops of the first floor dissipator

(c) Time-history of the input energy

Figure 6 Seismic performance of building B3-0.12g (x direction). EW component of the Lorca record

Table 3 presents relevant response magnitudes for the case considered in Figure 6. Second column contains the Park & Ang damage index [Park, Ang 1985]; next four columns display the input energy and the percentages of that energy that are dissipated by the structural damping, absorbed by the energy dissipative devices and causing additional structural damage, respectively. Figures from Table 3 confirm the conclusions derived from Figure 6 ...

Case	Park & Ang damage index	Input energy (kNm)	Energy dissipated by damping (%)	Energy absorbed by the dissipators (%)	Energy causing additional damage (%)
Bare frame	0.134	...			
Braced frame	0.029	...			
Protected frame	0.015	...			

7 Conclusions

This paper describes the initial steps of a research oriented at reducing the seismic vulnerability of wide-beam buildings in Spain using hysteretic energy dissipators. A number of prototype 3 and 6-story buildings are retrofitted with dissipative devices; the performance is evaluated in terms of the reduction of the dynamic response under a number of representative seismic inputs. Three cases are

compared: bare frame (building without any bracing), protected frame (building with dissipators) and braced frame (building with rigid connections instead of dissipators).

The preliminary obtained results seem to indicate that the use of hysteretic energy dissipative devices (protected frame) reduces significantly the seismic response, compared to the unprotected building (bare frame). Conversely, the comparison between the seismic performances of the protected frame and the braced frame is still unclear.

8 Acknowledgements

This paper has been financed by the Spanish Government under projects CGL2008-00869/BTE, CGL2011-2362, BIA2011-26816 and from the European Union (Feder); this support is gratefully acknowledged.

9 References

- [1] ACI 318-08 (2008): "Building Code Requirements for Structural Concrete and Commentary," American Concrete Institute.
- [2] Akiyama H. (1985): "Earthquake-resistant limit-state design for buildings", University of Tokyo Press, Tokyo.
- [3] Baber TT, Noori MN (1985): "Random Vibration of Degrading Pinching Systems," *Journal of Engineering Mechanics*, 111(8). 1010-1026.
- [4] Benavent-Climent A, Pujades LG, López-Almansa F (2002): "Design energy input spectra for moderate seismicity regions," *Earthquake Engineering & Structural Dynamics*, 31:1151–1172.
- [5] Benavent-Climent A (2007): "Seismic behavior of RC beam–column connections under dynamic loading," *Journal of Earthquake Engineering*, 11:493–511.
- [6] Benavent-Climent A, Cahís X, Vico JM (2009a): "Interior wide beam-column connections in existing RC frames subjected to lateral earthquake loading," Springer Science Business Media, B.V.
- [7] Benavent-Climent A, Cahís X, Zahran R (2009b): "Exterior wide beam column connections in existing RC frames subjected to lateral earthquake loads," *Engineering Structures*, 31 141-1424.
- [8] Benavent-Climent A, Zahran R (2010): "An energy-based procedure for the assessment of seismic capacity of existing frames: application to RC wide beam systems in Spain," *Soil Dynamics and Earthquake Engineering*, 30(5):354–367.
- [9] Benavent-Climent A (2011): An energy-based method for seismic retrofit of existing frames using hysteretic dampers. *Soil Dynamics and Earthquake Engineering* 31 1385–1396.
- [10] Benavent-Climent A, Donaire-Ávila J, Escobedo A, Oliver-Sáiz E, Ramírez-Márquez AL, Feriche M (2012): "Damage assessment on building structures subjected to the recent near-fault earthquake in Lorca (Spain)," 15th WCEE, Lisbon.
- [11] Benavent-Climent A, Escobedo A, Donaire-Ávila J, Oliver-Sáiz E, Ramírez-Márquez AL (2013): "Assessment of expected damage on buildings subjected to Lorca earthquake through an energy-based seismic index method and nonlinear dynamic response analyses," *Bulletin of Earthquake Engineering*, Pending.
- [12] Benavent-Climent A (2014): "Energy---based design of non---traditional structures incorporating hysteretic dampers: experimental validation with shaking table tests" 15ECEE (15th European Conference of Earthquake Engineering).
- [13] Bentz E, Collins MP (2000): Response-2000, V.1.0.5. Toronto University. Toronto, Ontario, Canada.
- [14] Domínguez D (2012): "Evaluación de la capacidad sismorresistente de edificios con vigas planas situados en zonas de España de sismicidad baja a moderada," Tesis Doctoral. Universidad Politécnica de Cataluña.
- [15] Domínguez D, López Almansa F, Benavent Climent A (2014): "Comportamiento, para el terremoto de Lorca de 11-05-2011, de edificios de vigas planas proyectados sin tener en cuenta la acción sísmica," *Informes de la Construcción*, Vol. 66, No. 553, e008.
- [16] EH-80 (1980): "Instrucción para el proyecto y ejecución de obras de hormigón en masa o armado," Ministerio de Fomento.

- [17] EHE (2008): "Instrucción de Hormigón Estructural," Ministerio de Fomento.
- [18] EN 1992 (Eurocode 2). (2003): "Design of Concrete Structures," European Committee for Normalization.
- [19] EN 1996 (Eurocode 6). (2005): "Design of Masonry Structures," European Committee for Normalization.
- [20] EN 1998 (Eurocode 8). (2005): "Design of Structures for Earthquake Resistance," European Committee for Normalization.
- [21] Foti D, Bozzo LM, López Almansa F. (1998): "Numerical Efficiency Assessment of Energy Dissipators for Seismic Protection of Buildings", *Earthquake Engineering & Structural Dynamics*. 27 543-556.
- [22] IGME (2011): "Informe geológico preliminar del terremoto de Lorca del 11 de mayo del año 2011, 5.1 Mw," Instituto Geológico y Minero de España.
- [23] IGN (2011): "Serie terremoto NE Lorca (Murcia) 11/05/2011," Instituto Geográfico Nacional.
- [24] Kunnath SK, Reinhorn AM (2010): "IDARC 2D Version 7.0. Program for the Inelastic Damage Analysis of Reinforced Concrete Structure," State University of New York at Buffalo.
- [25] López Almansa F, Domínguez D, Benavent Climent A (2013): "Seismic performance of RC buildings with wide beams," *Engineering Structures*, 46 687–702.
- [26] Manfredi G. (2001): Evaluation of seismic energy demand. *Earthquake Engineering & Structural Dynamics*. 30:1 485-499.
- [27] Martínez JL, Martín JA, León J (2001): "Comportamiento mecánico de la obra de fábrica. Monografía sobre el análisis estructural de construcciones históricas de fábrica," Universidad Politécnica de Madrid.
- [28] Masi A (2003): "Seismic Vulnerability Assessment of Gravity Load Designed R/C Frames," *Bulletin of Earthquake Engineering*, 1:371–395.
- [29] Mehrabi AB, Shing PB, Schuller MP, Noland JL (1994): "Performance of masonry-infilled RC frames under in-plane lateral loads," Report CD/SR-94/6. University of Colorado at Boulder.
- [30] Mostafaei H, Kabeyasawa T (2004): "Effect of Infill Masonry Walls on the Seismic Response of Reinforced Concrete Buildings," *Bulletin of the Earthquake Research Institute, University of Tokyo*. 79:133-156.
- [31] NCSE-94 (1994): "Norma de Construcción Sismorresistente", Ministerio de Fomento.
- [32] NCSE-02 (2002): "Norma de Construcción Sismorresistente," Ministerio de Fomento.
- [33] Newmark NM (1959): "A method of computation for structural dynamics," *Journal of Engineering Mechanics, ASCE*, 85(EM3), 67-94.
- [34] Paulay T, Priestley MJN (1992): *Seismic Design of Reinforced Concrete and Masonry Buildings*. Wiley.
- [35] Reinhorn AM, Roh H, Sivaselvan M, Kunnath SK, Vallés RE, Madan A, Li C, Lobo R, Park YJ (2009): "IDARC 2D Version 7.0. Program for the Inelastic Damage Analysis of Structures," MCEER Technical Report MCEER-09- 006. State University of New York at Buffalo.
- [36] Ricci P, de Risi MT, Verderame GM, Manfredi G (2013): "Influence of infill distribution and design typology on seismic performance of low- and mid-rise RC buildings," *Bulletin of Earthquake Engineering*, 11:5 1585-1616.
- [37] Sugano S (1968): "Study on inelastic stiffness of reinforced concrete structures," Research reports of the Annual Meeting of the Architectural Institute of Japan Kanto Branch. Tokyo, Japan, 3 25-32.